Demagnetizing Factors for Rectangular Prisms

D.-X. Chen[1], E. Pardo[2], and A. Sanchez[2]

[1]ICREA and Grup d'Electromagnetisme, Departament de Física, Universitat Autònoma de Barcelona, 08193 Bellaterra, Barcelona, Spain

[2]Grup d'Electromagnetisme, Departament de Física, Universitat Autònoma de Barcelona, 08193 Bellaterra, Barcelona, Spain

For rectangular prisms of dimensions $2a \times 2b \times 2c$ with constant material susceptibility χ, we have calculated and tabulated the fluxmetric and magnetometric demagnetizing factors N_f and N_m, defined along the $2c$ dimension as functions of $c/(ab)^{1/2}(=1 \sim 500)$, $a/b(=1 \sim 256)$, and $\chi(=0 \sim 10^9)$. We introduce an interpolation technique for obtaining $N_{f,m}$ with arbitrary values of $c/(ab)^{1/2}$, a/b, and χ.

***Index Terms*—Demagnetizing correction, fluxmetric demagnetizing factor, magnetometric demagnetizing factor, magnetic measurements, rectangular prisms.**

I. Introduction

When a body is placed in a uniform applied field $\mathbf{H}_a$, it is magnetized not only by $\mathbf{H}_a$ but also by the field produced by the resultant magnetic poles in the body itself. The field produced by such poles is usually called the demagnetizing field $\mathbf{H}_d$. Assuming the material to have a constant susceptibility χ for the sake of simplicity, the magnetic poles can be present only on the body surface and they appear only when there are some surfaces not parallel to the applied field. Since $\mathbf{H}_d$ and so the magnetization $\mathbf{M}$ are generally nonuniform and depend on both χ and body shape, the demagnetizing effects may bring about great complexities in the magnetic measurements of materials [1]–[3].

In order to avoid such effects, toroidal samples are recommended in magnetic measurements of soft and semi-soft magnetic materials. In this case, the sample is magnetized by a current- carrying coil uniformly wound on to it, so that the entire sample surface is parallel to the circular applied field and the demagnetizing field is absent at a sacrifice of the uniformity of the circular applied field, which is inversely proportional to the distance to the axis of cylindrical symmetry of the sample. The maximum circular field that can be applied is on the order of 10 kA/m, which is limited by the allowed maximum temperature rise. For semi-soft magnetic materials, one can use a permeameter to measure a single tape, whose both ends are well touched to a yoke made of soft-magnetic lamination, forming a closed magnetic circuit. When a uniformly wound current-carrying solenoid surrounds the tape, the demagnetizing fields produced by the poles appearing in both end regions will be partially cancelled by the fields produced by the poles induced in the yoke with signs opposite to those in the tape ends. The maximum field in such single tape measurements can be several times greater than that in ring sample measurements. For hard magnetic materials requiring a maximum field of the order of MA/m, the recommended sample shapes are cylinders or rectangular prisms and the magnetizer is usually an electromagnet. In this case, the fields produced by the induced poles in soft-magnetic pole pieces of the magnet will also reduce the demagnetizing field in the sample [1], [2].

In contrast to the above examples where demagnetizing fields are reduced or eliminated, there has been another way to deal with the demagnetizing problem in magnetic measurements, which is to calculate demagnetizing factors for certain sample shapes. In this case, the sample made of material with a constant susceptibility χ and having a certain symmetric shape is placed in a uniform $\mathbf{H}_a$, and if the average magnetization $\mathbf{M}_{\rm av}$ in the sample is parallel to $\mathbf{H}_a$ along the symmetry axis and so is the average demagnetizing field $\mathbf{H}_{d,\rm av}$, then the average demagnetizing factor $N_{\rm av}$ is defined as $\mathbf{H}_{\rm d,av} = -N_{\rm av}\mathbf{M}_{\rm av}$. If the body shape is ellipsoidal, $\mathbf{M}$ and $\mathbf{H}_d$ are uniform, so that $N_{\rm av}$ is reduced to a simple demagnetizing factor N, which is a function of the aspect ratios of the sample but independent of χ and was analytically calculated a long time ago [4]. For any other shapes, one has to define how the average is made and $N_{\rm av}$ will depend not only on aspect ratios but also on χ. Corresponding to magnetometric and fluxmetric measurements, the average is conventionally made over the entire body volume and over the midplane, and the $N_{\rm av}$'s are referred to as the magnetometric and fluxmetric demagnetizing factors, N_m and N_f, respectively [3]. If $N_{f,m}$ values are available, χ may be calculated from the directly measured external susceptibility $\chi_{\rm ex}$ of the sample, defined by $\mathbf{M}_{\rm av} = \chi_{\rm ex}\mathbf{H}_{\rm a}$. In fact, in the research and development of magnetic materials, wires, cylinders, and rectangular tapes and blocks are often the most convenient sample shapes, and they may be easily magnetized by a current-carrying solenoid, so that the calculation of demagnetizing factors is necessary in practice.

The numerical calculations of $N_{f,m}$ for different sample shapes with different aspect ratios and χ have formed a century old topic [3]. However, a practically complete set of results was obtained just a decade ago for one shape, cylinder, thanks to the developments of computer technology [3]. For another important geometry, rectangular prism, there have long been analytical results of $N_{f,m}$ for the general three-dimensional case for $\chi = 0$ and analytical transverse $N_{f,m}$ for infinitely long bars for $\chi = \infty$ [5]–[8]. For these latter bars, transverse $N_{f,m}$ as functions of χ and the transverse aspect ratio have been calculated recently [9], [10]. Since a complete functional three-dimensional calculation is too complicated, we have calculated the axial $N_{f,m}$ of square bars as functions of the aspect ratio and χ to compare with the existing results of cylinders,

Digital Object Identifier 10.1109/TMAG.2005.847634

and $N_{f,m}$ of rectangular prisms as functions of aspect ratios for the case of $\chi = -1$ for applications in superconductors [11], [12]. In the present paper, we will give $N_{f,m}$ of rectangular prisms as functions of aspect ratios and $\chi\ (\geq 0)$, relevant to the measurements of various magnetic materials. Different from the results given in [3], [10]–[12], where only tables of discrete data points are present and functional curves are plotted directly from the data in the tables, we will introduce an accurate interpolation technique in detail, so that the resultant $N_{f,m}$ are actually presented as continuous functions of aspect ratios and χ in a wide range. This will provide readers who need to make demagnetizing corrections for their sample having any values of aspect ratios and χ with relevant correct $N_{f,m}$. Moreover, we will introduce an iteration technique in detail, so that the final χ and $N_m(\chi)$ of the sample can be obtained from the directly measured $\chi_{\rm ex}$ and aspect ratios.

Although the method and formulas for the present calculations have already been given in [11] and [12], we will make a necessary description on them in Section II, commenting on the reasons for the steps and conditions we have used in this work. Although these reasons are stated in a logical way, they were not realized *a priori* but concluded from the success and failure of our long-term intensive work. Thus, we expect that such a description can be practically useful to those who are dealing with demagnetizing problems. The results of $N_{f,m}$ will be presented as tables and figures in Section III. Section IV will be devoted to the discussion and application of the results and our conclusions will be stated in Section V. In the Appendix, we summarize the quantities appearing in the paper for facilitating the readers.

II. Calculation

A. Magnetostatic Problem of Rectangular Prism

We consider a rectangular prism located at $-a \leq x \leq a, -b \leq y \leq b, -c \leq z \leq c$ with constant material susceptibility χ. The prism is immersed in a uniform applied field $\mathbf{H}_a$ in the z direction, as shown in Fig. 1(a). Since $\nabla \cdot \mathbf{B} = 0$ and $\mathbf{B} = \mu_0(1 + 1/\chi)\mathbf{M}$, we have $\nabla \cdot \mathbf{M} = 0$ inside the body, so that the volume pole density, which is proportional to $\nabla \cdot \mathbf{M}$, is zero. Thus, the magnetostatic problem is aimed to find the distribution of surface magnetic pole density, $\sigma(\mathbf{r})$.

The distribution of σ can be very different for different values of χ; it is constant on the end planes perpendicular to the applied field and null on the side planes when $\chi = 0$, but varies in inverse proportion to the $1/3$ power of the distance to each edge when $\chi \to \infty$ [9], [10]. In this case, a finite-element technique will be appropriate to use for all cases. With this technique, the entire surface of the prism is divided into n rectangular elements, each having a uniform pole density σ^i, and using $\sigma/\mu_0 = \mathbf{M}\cdot\mathbf{e} = \chi(\mathbf{H}_a + \mathbf{H}_d)\cdot\mathbf{e}$, $\mathbf{e}$ being the outward unit vector normal to the surface, and taking into account that σ is the only source of the local demagnetizing field $\mathbf{H}_d$, we find that

$$\frac{\sigma^i}{\chi\mu_0} + \sum_{j=1}^{n} \mathbf{e}^i \cdot \mathbf{D}^{ij} \frac{\sigma^j}{\mu_0} = \mathbf{e}^i \cdot \mathbf{H}_a \tag{1}$$

where $\mathbf{e}^i$ is the outward unit vector normal to the ith element and $\mathbf{D}^{ij}\sigma^j/\mu_0$ is the negative of the average demagnetizing field on the ith element generated by the jth element, which is calculated in Appendix A of [11] from the magnetic Coulomb law

$$\mathbf{H}(\mathbf{r}) = \frac{1}{4\pi\mu_0} \int_{S'} \frac{\sigma(\mathbf{r}')(\mathbf{r} - \mathbf{r}')}{|\mathbf{r} - \mathbf{r}'|^3}\, \mathrm{d}S' \tag{2}$$

where S' is the entire body surface and $\mathbf{r}'$ is a vector ending at this surface. Note that in this work we relate σ^i for all the elements using the local demagnetizing field $\mathbf{H}_d$ averaged over

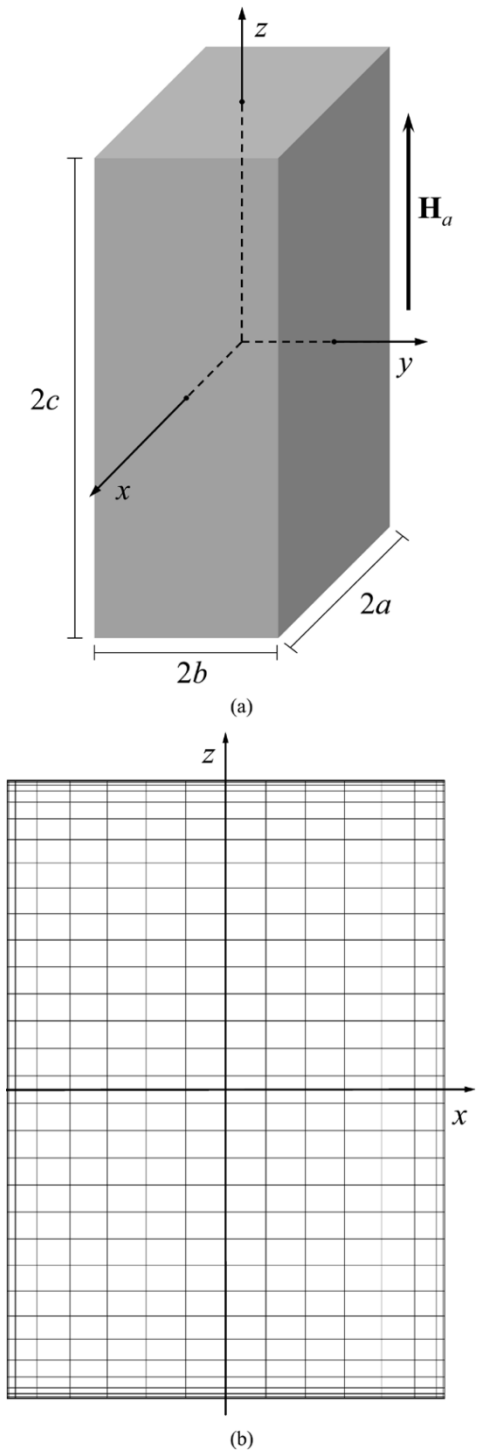

Fig. 1. (a) The studied prism with coordinates and applied field. (b) Element distribution on the side surface of $y = b$ for a prism of $\chi = 10^9$, $a/b = 2$, and $c/(ab)^{1/2} = 2$ calculated from (3) and (5) using $n_p = 256$.

the surface of each element, rather than using $\mathbf{H}_d$ at the center of each element as done in [3] and [10]. This modification allows us to improve appreciably the accuracy of calculated $N_{f,m}$ for prisms to a level higher than that for cylinders calculated in [3]. Otherwise, the pole distribution of a prism (having 12 edges) is much more difficult to be calculated accurately than that of a cylinder (having only two edges) [7], [13].

The set of linear equations (1) should include as many unknown variables σ^i as the number of elements covering the entire surface. However, as done in [10], the number of unknown variables can be reduced by considering the symmetry. To do so, we take σ^i for the elements within the $x, y, z > 0$ region as unknown variables and we include the contributions to $\mathbf{H}_d$ of the eight different elements at symmetric positions with the same magnitude of surface pole density in the matrix $\mathbf{D}^{ij}$. The resultant set of linear equations is solved using the LU decomposition routine [14].

B. Surface Element Division

The division of the surface into elements is done as follows. The elements are taken to be rectangular shaped. Their size in the z direction Δz depends only on the z coordinate of the position of the element center z_i, Δx depends only on x_i, and Δy depends only on y_i. In this way, the surface division into elements can be done as the composition of three independent line element divisions. We take the same nonlinear line division in the z direction as done in [10] for the direction parallel to the applied field. Consistently, the line divisions in the x and y directions are done as in [10] for the direction perpendicular to the field. A more detailed description is made as follows.

As derived in [9], when $\chi = \infty, \sigma$ tends to infinity as $-1/3$ power over the distance to the edge. Since $N_{f,m}$ at high χ are most difficult to be calculated accurately, the surface element distribution should be made based on this law. Improving the calculation for cylinders, where a basically uniform pole intensity for $\chi \to \infty$ is made in the elements near the edges, a roughly uniform pole-density increment for $\chi \to \infty$ is implemented near the edges for the present calculation. As in [10], we use artificial σ distributions

$$\sigma(x) = \left(1 - \frac{x}{a+\delta a}\right)^{-1/3} - \left(1 + \frac{x}{a+\delta a}\right)^{-1/3} + \frac{q_x x}{a+\delta a} \tag{3}$$

$$\sigma(y) = \left(1 - \frac{y}{b+\delta b}\right)^{-1/3} - \left(1 + \frac{y}{b+\delta b}\right)^{-1/3} + \frac{q_y y}{b+\delta b} \tag{4}$$

$$\sigma(z) = \left(1 - \frac{z}{c+\delta c}\right)^{-1/3} - \left(1 + \frac{z}{c+\delta c}\right)^{-1/3} + \frac{q_z z}{c+\delta c} \tag{5}$$

to calculate the element divisions along the x, y, and z directions, respectively. In order to overcome the difficulty arising from the actually infinite σ at the edges, we extend the a, b, and c for small lengths $\delta a, \delta b$, and δc, so that the $\sigma(a), \sigma(b)$, and $\sigma(c)$ calculated from (3)–(5) are large finite numbers. Thus, the division units become $\Delta\sigma_z = \sigma(z = c)/(n_z + 1/2), \Delta\sigma_x = \sigma(x = a)/n_x$, and $\Delta\sigma_y = \sigma(y = b)/n_y$. The proper values of $\delta a/a, \delta b/b, \delta c/c$, and $q_{x,y,z}$ are chosen for different values of χ and aspect ratios in such a way that the minimum error in the calculated $N_{f,m}$ is obtained.

The numbers of divisions in the three directions, $2n_x, 2n_y$, and $2n_z+1$ (with a layer riding on the $z = 0$ midplane with $\sigma = 0$, which is essential for reducing the error of the final results, especially for N_f), are taken by fixing the number of elements integrally belonging to the $x, y, z > 0$ region, n_p [$\equiv n_x n_y + n_x n_z + n_y n_z = (n - 4n_x - 4n_y)/8$], selecting $n_x = n_y$ (this is tested to be a proper choice independent of the value of a/b), and assuming $n_z/n_x \approx c/\sqrt{ab}$. The elements centered at $z = 0$ have $\sigma^i = 0$, so that σ^i on these elements are not unknown variables. We also consider a restriction for $n_x, n_y \geq (\sqrt{n_p/3})/5$. This restriction ensures sufficiently fine divisions when $c/\sqrt{ab}$ is very large so that a minimum error in the final $N_{f,m}$ is reached.

An exemplified element division on a side surface for a prism of $\chi = 10^9, a/b = 2$, and $c/(ab)^{1/2} = 2$ is shown in Fig. 1(b). In order to have a sufficient resolution near the edges, $n_p = 256$ is used with $n_x = n_y = 8$ and $n_z = 16$. In the actual calculation, n_p is set as large as 4800.

C. Calculation of $N_{f,m}$

The fluxmetric and magnetometric demagnetizing factors, N_f and N_m, are defined by [3]

$$N_{f,m} = -H_{d,\mathrm{mid,vol}}/M_{\mathrm{mid,vol}} \tag{6}$$

where the subscripts "mid" and "vol" stand for the average over the midplane and over the entire volume, respectively. When the prism material has a constant χ as in the present case, the demagnetizing factors can be calculated from either $M_{\mathrm{mid,vol}}$ or $H_{d,\mathrm{mid,vol}}$ using [10]

$$N_{f,m} = \frac{H_a}{M_{\mathrm{mid,vol}}} - \frac{1}{\chi} \tag{7}$$

$$N_{f,m} = \frac{-H_{d,\mathrm{mid,vol}}}{\chi(H_{d,\mathrm{mid,vol}} + H_a)}. \tag{8}$$

Using the calculated surface pole density, $M_{\mathrm{mid,vol}}$ can be easily calculated by the surface integration of σ, using $\nabla \cdot \mathbf{M} = 0$ inside the body and $\mu_0 \mathbf{e} \cdot \mathbf{M} = \sigma$ on the surface [3], [10].

$H_{d,\mathrm{mid,vol}}$ may be calculated from the sum of the prism-midplane (at $z = 0$) and prism-volume averaged fields generated by all rectangular elements as

$$H_{d,\mathrm{mid}} = 8 \sum_{i=1}^{n_p} \frac{\sigma^i}{\mu_0} h^i_{z,\mathrm{mid}} \tag{9}$$

$$H_{d,\mathrm{vol}} = 8 \sum_{i=1}^{n_p} \frac{\sigma^i}{\mu_0} h^i_{z,\mathrm{vol}} \tag{10}$$

where $h^i_{z,\mathrm{mid}}$ and $h^i_{z,\mathrm{vol}}$ are the prism-midplane average and prism-volume average of the z component of the magnetic field per unit σ^i/μ_0 generated by the ith element at $x, y, z > 0$, whose analytical expressions may be obtained from the formulas derived in Appendixes A and B of [11]. The use of analytical formulas for $h^i_{z,\mathrm{mid,vol}}$ avoids doing numerical midplane and volume integrations, as done in [3], [10], so it avoids possible extra numerical error for $H_{d,\mathrm{mid,vol}}$ calculations and saves around 50% of the total computer time.

D. Correction of $N_{f,m}$

The demagnetizing factors $N_{f,m}$ can be calculated from either $M_{\mathrm{mid,vol}}$ or $H_{d,\mathrm{mid,vol}}$ using (7) and (8), respectively. If $N_{f,m}$ is calculated in both ways, we can obtain a corrected $N^c_{f,m}$. The correction formula is

$$N^c_{f,m} = N^v_{f,m}(1 + N^s_{f,m}\chi)\,/(1 + N^v_{f,m}\chi) \qquad (11)$$

where $N^s_{f,m}$ is the value of $N_{f,m}$ calculated using $M_{\mathrm{mid,vol}}$ and $N^v_{f,m}$ is obtained by means of $H_{d,\mathrm{mid,vol}}$.

Using the finite-element method, there is always a discretization error in the calculated pole density distribution, especially when χ is large so that σ shows a sharp divergence near the edges. When calculating $N_{f,m}$ of cylinders [3], we found that the calculated $N_{f,m}$ were very sensitive to the element division and that $N^s_{f,m}$ and $N^v_{f,m}$ calculated from the same σ distribution could be orders of magnitude different from each other even if quite a large element number was used. This became a vital problem that seriously limited the accuracy of the results of $N_{f,m}$. After carefully investigating (7) and (8), we found that a small error in $M_{\mathrm{mid,vol}}$ and $H_{d,\mathrm{mid,vol}}$ could result in a great error in $N^s_{f,m}$ and $N^v_{f,m}$. Then, reasonably assuming the relative errors in the calculated $M_{\mathrm{mid,vol}}$ and $H_{d,\mathrm{mid,vol}}$ owing to the discretization in the pole distribution to be the same

$$M_{\mathrm{mid,vol}}/M^*_{\mathrm{mid,vol}} = H_{d,\mathrm{mid,vol}}/H^*_{d,\mathrm{mid,vol}} \qquad (12)$$

where quantities with a superscript * denote their ideal correct values whereas those without a superscript denote their calculated values with some error, a correction formula (11) was derived from (7) and (8). Compared with the directly calculated $N^s_{f,m}$ and $N^v_{f,m}$, the error of the corrected $N^c_{f,m}$ was at least one order of magnitude smaller. The validity of such a correction technique has been further justified in [10] and used in [11], [12]. In the present work, all the final data for $N_{f,m}$ are actually $N^c_{f,m}$.

E. Error Estimation

In a previous work [10], the error in the calculated $N_{f,m}$ was checked by comparing the results with those calculated analytically for several χ values. However, for the case of prisms there are only exact analytical formulas for $N_{f,m}$ for $\chi = 0$ [5], [6]. Moreover, since the error for $\chi = \infty$ is at least one order of magnitude greater than that for $\chi = 0$ [10], these analytical formulas are useless for estimating the error for arbitrary χ. Consequently, an alternative error estimation method is applied.

The error involved in finite-element methods is mainly due to the division of a continuous body into discrete elements. The discretization error of the calculated σ^i decreases with increasing the number of elements n_p, so that the limit of $n_p \to \infty$ would yield to the exact σ^i, and consequently, the precise solution of $N_{f,m}$. Then, if we plot $N_{f,m}$ as a function of $1/n_p$, the exact $N_{f,m}$ value would correspond to $1/n_p = 0$. Furthermore, if $1/n_p$ is low enough, the $N_{f,m}$ dependence on $1/n_p$ could be assumed linear as a first approximation.

The error is estimated as follows. For each pair of χ and $c/\sqrt{ab}$ values, two $N_{f,m}$ calculations are done using different numbers of elements, $n_p^{(1)}$ and $n_p^{(2)}$ with $n_p^{(1)} > n_p^{(2)}$. Then, we regard the "exact" $N_{f,m}$ value as the linear extrapolation of $N_{f,m}(1/n_p)$ at $1/n_p = 0$, obtained from $N_{f,m}(1/n_p^{(1)})$ and $N_{f,m}(1/n_p^{(2)})$. Finally, the relative error of $N_{f,m}$ is estimated as $[N_{f,m}(1/n_p^{(1)}) - N_{f,m}(1/n_p = 0)]/[N_{f,m}(1/n_p = 0)]$, taking $N_{f,m}(1/n_p^{(1)})$ as the final $N_{f,m}$ value. For the calculations presented in this paper we have used $n_p^{(1)}$ being around 4800 and $n_p^{(2)}$ around 3700.

If the $1/n_p$ dependence of $N_{f,m}$ were exactly linear, we should use the extrapolated $N_{f,m}(1/n_p \to 0)$ as the final result. However, this is not the case, and we can only use this technique to estimate the error roughly.

III. Results

$N_{f,m}$ are calculated as functions of χ and aspect ratios of the prism. The three dimensions $2a, 2b$, and $2c$ should give two independent aspect ratios, and following the early numerical calculations of $N_{f,m}$ for $\chi = 0$ in [7], we choose them as a/b and $c/\sqrt{ab}$. The values of a/b are chosen with logarithmic uniformity as 1, 2, 4, 8, 16, 32, 64, 128, and 256, which are the same as those in [7]. The values of $c/\sqrt{ab}$ are chosen as 1, 1.5, 2, 5, 10, 20, 50, 100, 200, and 500. We omit data for $c/\sqrt{ab} < 1$ because long samples are more important in measurements of magnetic materials, which are our concern in the present work; the maximum $c/\sqrt{ab}$ is chosen as 500, since the calculated $N_{f,m}$ at $c/\sqrt{ab} > 500$ have too large error. Moreover, from the data points at these values of $c/\sqrt{ab}$, quite accurate continuous $N_{f,m}$ versus $c/\sqrt{ab}$ curves may be drawn using a spline line in logarithmic scales for each pair of values of χ and a/b. The values of χ were chosen quite arbitrarily when $N_{f,m}$ for cylinders were calculated in [3]; after studied the conjugate relations in [9] and [10], we now choose $\chi = 10^{-4}, 1.5, 9, 99, 999, 9999, 10^5$, and 10^9. These values include the extreme value $10^9 \sim \infty$ and $10^{-4} \sim 0$, where analytical exact $N_{f,m}$ are known. Since a complete calculation of demagnetizing factors of prisms involves a huge amount of computation time, the above choice for calculation points aims to ensure that well distributed data points of $N_{f,m}$ with high accuracy can be used for as many cases as possible by accurate interpolation and extrapolation.

The obtained data for N_m and N_f are listed in Tables I and II, respectively. Since in magnetic measurements of samples with a high χ, the demagnetizing correction can be properly done only when their $c/(ab)^{1/2}$ is high enough, data for $\chi = 9999$ and 10^5 are given at high $c/(ab)^{1/2}$ only, although the results for the high χ limit are complete. The estimated errors are classified between $<0.01\%$ and $<3.1\%$, which are indicated by the numbers of significant digits and stars. N_m and N_f versus $c/(ab)^{1/2}$ curves for different values of a/b are plotted by spline lines in Figs. 2 and 3 for $\chi = 0, 1.5, 9, 99, 999$, and 10^9. We introduce grid lines so that values of $N_{f,m}$ can be easily estimated from the figures.

IV. Discussion

A. Variations of $N_{f,m}$ With Aspect Ratios and χ

A general description of the variations of $N_{f,m}$ with aspect ratio and χ was first given in [3] for cylinders. After calculating $N_{f,m}$ of square bars, their similarity to cylinders was shown in [11]. For infinitely long rectangular bars [9], [10], the behavior of transverse $N_{f,m}$ was found also to be basically similar to that

TABLE I

N_m OF RECTANGULAR PRISM $2a \times 2b \times 2c$ ALONG THE $2c$ DIMENSION AS A FUNCTION OF SUSCEPTIBILITY χ AND ASPECT RATIOS a/b AND $c/\sqrt{ab}$. THE ESTIMATED ERROR: $\chi = 0$, EXACT; SIX SIGNIFICANT DIGITS, $<0.01\%$; FIVE SIGNIFICANT DIGITS, $<0.1\%$; FOUR SIGNIFICANT DIGITS WITHOUT *, $<0.5\%$; WITH *, $<1\%$; WITH **, $<2.1\%$

χ	$c/\sqrt{ab}$	$a/b=1$	2	4	8	16	32	64	128	256
0	1	0.333333	0.322611	0.293917	0.254916	0.212988	0.173109	0.137855	0.108116	0.0838084
	1.5	0.249185	0.241036	0.219217	0.189567	0.157754	0.127615	0.101112	0.0788928	0.0608493
	2	0.198316	0.191906	0.174684	0.151161	0.125796	0.101682	0.0804438	0.0626410	0.0482041
	5	0.0883157	0.0856380	0.0783961	0.0683740	0.0573689	0.0466901	0.0371032	0.0289443	0.0222617
	10	0.0457312	0.0443880	0.0407521	0.0357101	0.0301516	0.0247212	0.0197963	0.0155508	0.0120259
	20	0.0232623	0.0225904	0.0207715	0.0182484	0.0154648	0.0127416	0.0102650	0.00811951	0.00632416
	50	0.00940036	0.00913159	0.00840396	0.00739459	0.00628094	0.00519117	0.00419962	0.00333968	0.00261848
	100	0.00471609	0.00458171	0.00421789	0.00371320	0.00315637	0.00261147	0.00211567	0.00168564	0.00132492
	200	0.00236203	0.00229483	0.00211292	0.00186058	0.00158216	0.00130971	0.00106181	8.4679E-4	6.66426E-4
	500	9.45765E-4	9.18888E-4	8.46125E-4	7.45186E-4	6.3382E-4	5.2484E-4	4.25678E-4	3.39671E-4	2.67525E-4
1.5	1	0.310299	0.300724	0.274693	0.238583	0.199141	0.161321	0.127857	0.099745	0.076942
	1.5	0.228419	0.221348	0.202057	0.175156	0.145743	0.117632	0.0928852	0.072220	0.055538
	2	0.179370	0.173953	0.159080	0.138177	0.115143	0.0929988	0.0734432	0.057081	0.043861
	5	0.0758983	0.0738819	0.0682711	0.0601855	0.0509654	0.0417661	0.0333571	0.0261212	0.0201542
	10	0.0380281	0.0370978	0.0344939	0.0306987	0.0263036	0.0218335	0.0176562	0.0139773	0.0108759
	20	0.0189510	0.0185089	0.0172676	0.0154493	0.0133292	0.0111553	0.00910433	0.00727751	0.00571660
	50	0.0075558	0.00738457	0.00690306	0.00619577	0.00536816	0.00451610	0.0037088	0.00298626	0.00236545
	100	0.00377300	0.00368832	0.00345009	0.00309985	0.00268955	0.00226660	0.00186533	0.00150578	0.00119646
	200	0.00188522	0.0018431	0.00172463	0.00155036	0.00134609	0.00113539	9.3537E-4	7.56035E-4	6.01678E-4
	500	7.53782E-4	7.36991E-4	6.89747E-4	6.20242E-4	5.38746E-4	4.5465E-4	3.7479E-4	3.03166E-4	2.41497E-4
9	1	0.287127	0.278799	0.255805	0.223131	0.186553	0.150786	0.118756	0.091750	0.069931
	1.5	0.208878	0.202666	0.185673	0.161482	0.134425	0.108107	0.084734	0.065218	0.049589
	2	0.161997	0.157284	0.144236	0.125601	0.104663	0.0842213	0.066037	0.050854	0.038698
	5	0.0637660	0.0621473	0.0576283	0.0510557	0.0434518	0.0357342	0.028579	0.022377	0.017253
	10	0.0295609	0.0289204	0.0271132	0.0244333	0.0212440	0.0178881	0.0146437	0.0117048	0.0091762
	20	0.0138366	0.013573	0.012823	0.011693	0.010320	0.0088388	0.00736654	0.00599339	0.00477604
	50	0.0052791	0.0051871	0.0049235	0.0045228	0.0040293	0.0034889	0.0029432	0.0024260	0.0019599
	100	0.0025962	0.0025523	0.0024262	0.0022339	0.0019962	0.0017347	0.0014693	0.00121663	9.87797E-4
	200	0.0012873	0.0012658	0.0012042	0.0011100	9.9338E-4	8.6476E-4	7.3395E-4	6.09082E-4	4.95768E-4
	500	5.1237E-4	5.0388E-4	4.7954E-4	4.4234E-4	3.9620E-4	3.4527E-4	2.9339E-4	2.43801E-4	1.9874E-4
99	1	0.27593	0.26811	0.24644	0.21541	0.18032	0.14564	0.114291	0.087671	0.066072
	1.5	0.19996	0.19397	0.17771	0.15455	0.12852	0.10304	0.0802464	0.061117	0.045782
	2	0.15427	0.14971	0.13710	0.11913	0.098943	0.079194	0.0615596	0.0468027	0.035009
	5	0.057845	0.056276	0.051911	0.045603	0.038393	0.031188	0.024606	0.018967	0.014366
	10	0.0241785	0.023614	0.022028	0.019698	0.016971	0.014160	0.011499	0.0091241	0.0070999
	20	0.00955902	0.0093767	0.0088592	0.0080857	0.0071558	0.006164	0.005184	0.004265	0.0034374
	50	0.0029361	0.0028938	0.0027722	0.002586	0.002355	0.002097	0.001829	0.001562	0.001307
	100	0.0013161	0.00129955	0.00125162	0.0011774	0.0010836	9.771E-4	8.636E-4	7.4821E-4	6.3522E-4
	200	6.2314E-4	6.1580E-4	5.9452E-4	5.6141E-4	5.1924E-4	4.7087E-4	4.1885E-4	3.6538E-4	3.1245E-4
	500	2.4132E-4	2.3858E-4	2.3065E-4	2.1825E-4	2.0241E-4	1.8415E-4	1.6442E-4	1.4400E-4	1.2366E-4
999	1	0.27460	0.26683	0.24530	0.21445	0.17953	0.14498	0.113716	0.0871384	0.065552
	1.5	0.19893	0.19295	0.17676	0.15368	0.12775	0.10235	0.0796218	0.0605299	0.045213
	2	0.15339	0.14884	0.13625	0.11831	0.098177	0.078483	0.060897	0.0461766	0.0344074
	5	0.057134	0.055564	0.051192	0.044873	0.037652	0.030442	0.023873	0.018268	0.013711
	10	0.0233930	0.022831	0.021252	0.018932	0.016216	0.01342	0.01078	0.008448	0.006478
	20	0.00869446	0.0085190	0.0080215	0.0072793	0.006390	0.005446	0.004521	0.003664	0.002906
	50	0.0021625	0.0021291	0.0020335	0.001889	0.001711	0.001517	0.001317*	0.001122*	9.379E-4*
	100	7.6877E-4	7.5934E-4	7.3222E-4	6.9070E-4	6.3890E-4	5.807E-4	5.194E-4	4.571E-4	3.957E-4
	200	3.028E-4	2.998E-4	2.911E-4	2.777E-4	2.607E-4	2.4116E-4	2.1997E-4	1.97791E-4	1.7519E-4
	500	1.040E-4*	1.031E-4*	1.005E-4*	9.648E-5*	9.134E-5*	8.535E-5*	7.878E-5*	7.173E-5*	6.440E-5
9999	10	0.0233099	0.022748	0.021169	0.01885	0.016133	0.01334	0.01070	0.004977	0.006396
	20	0.00859579	0.0084209	0.0079247	0.0071857	0.006298	0.005356	0.004434	0.002155	0.002824
	50	0.0020485	0.0020158	0.0019222	0.001781	0.001607	0.001418	0.001224*	6.235E-4*	8.576E-4**
	100	6.5602E-4	6.4730E-4	6.22313E-4	5.8427E-4	5.372E-4	4.848E-4	4.301E-4	2.155E-4	3.219E-4
	200	2.092E-4	2.0694E-4	2.0036E-4	1.9030E-4	1.7772E-4	1.6357E-4	1.4856E-4	6.465E-5	1.178E-4
	500	5.159E-5*	5.113E-5*	4.988E-5*	4.795E-5*	4.553E-5*	4.278E-5*	3.984E-5**	8.899E-6*	3.353E-5*
1E5	100	6.4297E-4	6.3430E-4	6.09474E-4	5.7170E-4	5.249E-4	4.730E-4	4.189E-4	3.646E-4	3.119E-4*
	200	1.9589E-4	1.9364E-4	1.8722E-4	1.77414E-4	1.6519E-4	1.515E-4	1.370E-4	1.222E-4	1.075E-4
	500	4.001E-5	3.963E-5	3.855E-5	3.690E-5	3.483E-5	3.251E-5	3.003E-5	2.746E-5	2.486E-5
1E9	1	0.27445	0.26669	0.24517	0.21434	0.17944	0.14491	0.11365	0.0870765	0.065492
	1.5	0.19882	0.19283	0.17665	0.15358	0.12766	0.10227	0.0795486	0.0604605	0.045145
	2	0.15329	0.14874	0.13615	0.11822	0.098088	0.078399	0.060818	0.0461013	0.0343343
	5	0.057053	0.055483	0.051110	0.044789	0.037565	0.030353	0.023783	0.01818	0.01362
	10	0.0233006	0.022739	0.021160	0.018841	0.016124	0.01333	0.01069	0.008354	0.006386
	20	0.00858466	0.0084098	0.0079138	0.0071738	0.006287	0.005346	0.004424	0.003570	0.002815
	50	0.0020351	0.0020024	0.0019091	0.001768	0.001595	0.001406	0.001213*	0.001024*	8.473E-4**
	100	6.4149E-4	6.3282E-4	6.0802E-4	5.7027E-4	5.235E-4	4.717E-4	4.176E-4	3.634E-4	3.107E-4*
	200	1.9433E-4	1.9208E-4	1.8568E-4	1.75896E-4	1.6371E-4	1.500E-4	1.356E-4	1.209E-4	1.062E-4
	500	3.8443E-5	3.8069E-5	3.702E-5	3.5385E-5	3.3353E-5	3.1058E-5	2.863E-5	2.610E-5	

of cylinders. For a general rectangular prism like in the present case, $N_{f,m}$ at $1 \leq a/b \leq 256$ and $0.001 \leq c/(ab)^{1/2} \leq 1000$ were discussed in [7] for $\chi = 0$. Extending the calculations to $\chi \geq 0$ and $c/(ab)^{1/2} \geq 1$, we can observe from comparing our

TABLE II

N_f OF RECTANGULAR PRISM $2a \times 2b \times 2c$ ALONG THE $2c$ DIMENSION AS A FUNCTION OF SUSCEPTIBILITY χ AND ASPECT RATIOS a/b AND $c/\sqrt{ab}$. THE ESTIMATED ERROR: $\chi = 0$, EXACT; SIX SIGNIFICANT DIGITS, $<0.01\%$; FIVE SIGNIFICANT DIGITS, $<0.1\%$; FOUR SIGNIFICANT DIGITS WITHOUT *, $<0.5\%$; WITH *, $<1\%$; WITH **, $<2.1\%$; WITH ***, $<3.1\%$

χ	$c/\sqrt{ab}$	$a/b=1$	2	4	8	16	32	64	128	256
0	1	0.258730	0.246476	0.214786	0.174455	0.134840	0.100896	0.0739757	0.0535548	0.0384634
	1.5	0.163927	0.156148	0.136195	0.111023	0.0863536	0.0651013	0.0480792	0.0350252	0.0252817
	2	0.110890	0.106172	0.0938227	0.0777385	0.0614247	0.0469312	0.0350283	0.0257229	0.0186773
	5	0.0236312	0.0232633	0.0221282	0.0202017	0.0176052	0.0146461	0.0116953	0.00903655	0.00681014
	10	0.00624236	0.00621320	0.00611520	0.00591797	0.00557962	0.00507133	0.00440998	0.00366497	0.00292514
	20	0.00158365	0.00158170	0.00157497	0.00156045	0.00153229	0.00148115	0.00139566	0.00126816	0.00110263
	50	2.54444E-4	2.54394E-4	2.54216E-4	2.53826E-4	2.53032E-4	2.51466E-4	2.48441E-4	2.42795E-4	2.32846E-4
	100	6.36492E-5	6.36461E-5	6.36349E-5	6.36103E-5	6.356E-5	6.34594E-5	6.32596E-5	6.28673E-5	6.21107E-5
	200	1.59147E-5	1.59145E-5	1.59138E-5	1.59123E-5	1.59091E-5	1.59028E-5	1.58901E-5	1.58649E-5	1.58149E-5
	500	2.54646E-6	2.54646E-6	2.54644E-6	2.54639E-6	2.54632E-6	2.54616E-6	2.54583E-6	2.54517E-6	2.54387E-6
1.5	1	0.254263	0.244390	0.217939	0.182217	0.144593	0.110133	0.0813262	0.058744	0.041815
	1.5	0.168735	0.162223	0.144583	0.120474	0.0950263	0.0719052	0.052837	0.038077	0.027121
	2	0.119590	0.115197	0.103129	0.0863337	0.0683546	0.0519011	0.0382795	0.0277109	0.0198357
	5	0.0290206	0.0282899	0.0262411	0.0232122	0.0196209	0.0159038	0.0124391	0.00945988	0.00704487
	10	0.00744621	0.00735140	0.00707910	0.00665360	0.00609137	0.00540084	0.00460951	0.00378028	0.00298960
	20	0.00174016	0.00173276	0.00171082	0.00167426	0.00162096	0.00154529	0.00143878	0.00129525	0.00111871
	50	2.62774E-4	2.62528E-4	2.61800E-4	2.6059E-4	2.58816E-4	2.56201E-4	2.52137E-4	2.45524E-4	2.34738E-4
	100	6.4566E-5	6.4543E-5	6.44764E-5	6.43698E-5	6.42222E-5	6.40191E-5	6.37189E-5	6.32323E-5	6.23898E-5
	200	1.60192E-5	1.6017E-5	1.6010E-5	1.5999E-5	1.59851E-5	1.59675E-5	1.59439E-5	1.59087E-5	1.58499E-5
	500	2.55266E-6	2.5521E-6	2.5523E-6	2.5517E-6	2.5510E-6	2.5503E-6	2.5490E-6	2.5477E-6	2.54605E-6
9	1	0.247249	0.239217	0.217170	0.186176	0.151989	0.119160	0.0903811	0.066743	0.048195
	1.5	0.170938	0.165286	0.149819	0.127923	0.103696	0.0805140	0.060397	0.044068	0.031478
	2	0.126508	0.122399	0.111033	0.0948505	0.0768183	0.0594935	0.044434	0.032275	0.022967
	5	0.038050	0.036929	0.033825	0.029362	0.024281	0.019223	0.014658	0.010856	0.0078792
	10	0.011244	0.010968	0.010204	0.0091083	0.0078547	0.0065740	0.0053437	0.0042180	0.00324077
	20	0.0024650	0.0024282	0.0023261	0.0021780	0.0020038	0.0018159	0.0016175	0.0014064	0.00118449
	50	2.9792E-4	2.9688E-4	2.9393E-4	2.8937E-4	2.8353E-4	2.7649E-4	2.6797E-4	2.5718E-4	2.4279E-4
	100	6.79458E-5	6.78671E-5	6.76419E-5	6.72907E-5	6.68357E-5	6.6285E-5	6.56195E-5	6.47685E-5	6.3578E-5
	200	1.6377E-5	1.6368E-5	1.6346E-5	1.6311E-5	1.6268E-5	1.62174E-5	1.6158E-5	1.6088E-5	1.600E-5
	500	2.5719E-6	2.567E-6*	2.574E-6*	2.571E-6	2.568E-6	2.565E-6	2.561E-6	2.5579E-6	2.556E-6
99	1	0.24285	0.23547	0.21510	0.18621	0.15400	0.12267	0.0948412	0.071655	0.053116
	1.5	0.17096	0.16554	0.15086	0.13010	0.10703	0.084726	0.065084	0.048802	0.035920
	2	0.12900	0.12499	0.11394	0.098280	0.080838	0.063961	0.049038	0.036687	0.026924
	5	0.044368	0.043130	0.039688	0.034697	0.028990	0.023288	0.018086	0.013644	0.010041
	10	0.016655	0.016246	0.015098	0.013410	0.011432	0.009394	0.007468	0.005759	0.004316
	20	0.0052275	0.0051132	0.0047911	0.0043140	0.003748	0.003155	0.002584	0.002064	0.001609
	50	7.1703E-4	7.037E-4	6.666E-4	6.125E-4	5.498E-4	4.854E-4	4.241E-4*	3.679E-4*	3.170E-4
	100	1.094E-4	1.083E-4	1.052E-4	1.008E-4	9.569E-5	9.040E-5	8.521E-5	8.019E-5	7.524E-5
	200	1.9358E-5	1.9306E-5	1.9162E-5	1.8941E-5	1.8671E-5	1.8368E-5	1.804E-5	1.770E-5	1.734E-5
	500	2.704E-6	2.695E-6*	2.703E-6**	2.689E-6	2.682E-6*	2.664E-6	2.653E-6	2.632E-6	2.633E-6**
999	1	0.24229	0.23496	0.21477	0.18611	0.15413	0.12300	0.095324	0.072250	0.053783
	1.5	0.17091	0.16551	0.15091	0.13026	0.10733	0.085164	0.065636	0.049437	0.036607
	2	0.12925	0.12525	0.11423	0.098624	0.081257	0.064469	0.049626	0.037338	0.027614
	5	0.045218	0.043973	0.040514	0.035491	0.029744	0.024003	0.01877	0.01431	0.01069
	10	0.017674	0.017256	0.016083	0.014353	0.012315	0.01020	0.008199	0.006412	0.004896
	20	0.0062159	0.0060924	0.0057425	0.0052188	0.004588	0.003913	0.003246	0.0026232	0.002066
	50	0.0013244	0.0013027	0.001241	0.001147	0.001032	9.067E-4	7.786E-4*	6.5384E-4*	5.368E-4**
	100	3.3478E-4	3.2957E-4	3.1475E-4	2.924E-4	2.651E-4	2.354E-4	2.052E-4*	1.760E-4*	1.485E-4*
	200	5.839E-5	5.754E-5	5.509E-5	5.147E-5*	4.717E-5*	4.262E-5*	3.811E-5*	3.391E-5**	3.008E-5**
	500	3.833E-6*	3.810E-6**	3.768E-6*	3.695E-6*	3.591E-6**	3.490E-6**	3.381E-6*	3.283E-6*	3.185E-6*
9999	10	0.017784	0.017366	0.016191	0.014458	0.012416	0.01030	0.008289	0.006497	0.008364
	20	0.0063369	0.0062128	0.0058613	0.0053350	0.004700	0.004021	0.003348	0.002718	0.003580*
	50	0.0014448	0.0014225	0.001359	0.001263	0.001145	0.001015	8.806E-4	7.488E-4*	0.001035**
	100	4.3731E-4	4.3152E-4	4.1498E-4	3.8979E-4	3.5860E-4	3.239E-4	2.876E-4	2.511E-4	3.753E-4*
	200	1.207E-4	1.193E-4	1.1501E-4	1.087E-4	1.009E-4	9.2182E-5	8.304E-5	7.380E-5*	1.332E-4*
	500	1.575E-5	1.558E-5*	1.506E-5*	1.429E-5**	1.333E-5**	1.227E-5**	1.113E-5***	1.002E-5***	3.673E-5***
1E5	100	4.5046E-4	4.4464E-4	4.2801E-4	4.0265E-4	3.71307E-4	3.3631E-4	2.997E-4	2.629E-4	2.268E-4*
	200	1.331E-4	1.316E-4	1.273E-4	1.208E-4	1.127E-4	1.037E-4	9.4250E-5	8.462E-5	7.501E-5
	500	2.418E-5**	2.391E-5**	2.323E-5**	2.224E-5**	2.104E-5**	1.971E-5*	1.827E-5	1.6792E-5	1.527E-5
1E9	1	0.24222	0.23491	0.21473	0.18610	0.15414	0.12304	0.095378	0.072317	0.053859
	1.5	0.17091	0.16551	0.15091	0.13028	0.10736	0.085213	0.065698	0.049509	0.036686
	2	0.12928	0.12528	0.11426	0.098662	0.081304	0.064526	0.049693	0.037413	0.027695
	5	0.045316	0.044071	0.040609	0.035583	0.029833	0.024088	0.01886	0.01440	0.01078
	10	0.017800	0.017379	0.016203	0.014469	0.012427	0.01031	0.008299	0.006506	0.004986
	20	0.0063507	0.0062265	0.0058748	0.0053482	0.004713	0.004033	0.003360	0.002730	0.002166*
	50	0.0014594	0.0014371	0.001373	0.001277	0.001159	0.001028	8.939E-4*	7.616E-4*	6.357E-4**
	100	4.5196E-4	4.4614E-4	4.2951E-4	4.0417E-4	3.7277E-4	3.3775E-4	3.011E-4	2.642E-4	2.289E-4*
	200	1.346E-4	1.331E-4	1.288E-4	1.223E-4	1.142E-4	1.052E-4	9.5658E-5	8.601E-5	7.636E-5
	500	2.553E-5**	2.524E-5**	2.454E-5**	2.355E-5**	2.233E-5**	2.098E-5**	1.952E-5	1.804E-5	1.674E-5**

results with those given in [7] how $N_{f,m}$ change with increasing χ at $c/(ab)^{1/2} \geq 1$.

Looking at the curves plotted in Figs. 2 and 3 and calculating from the data listed in Tables I and II, we see

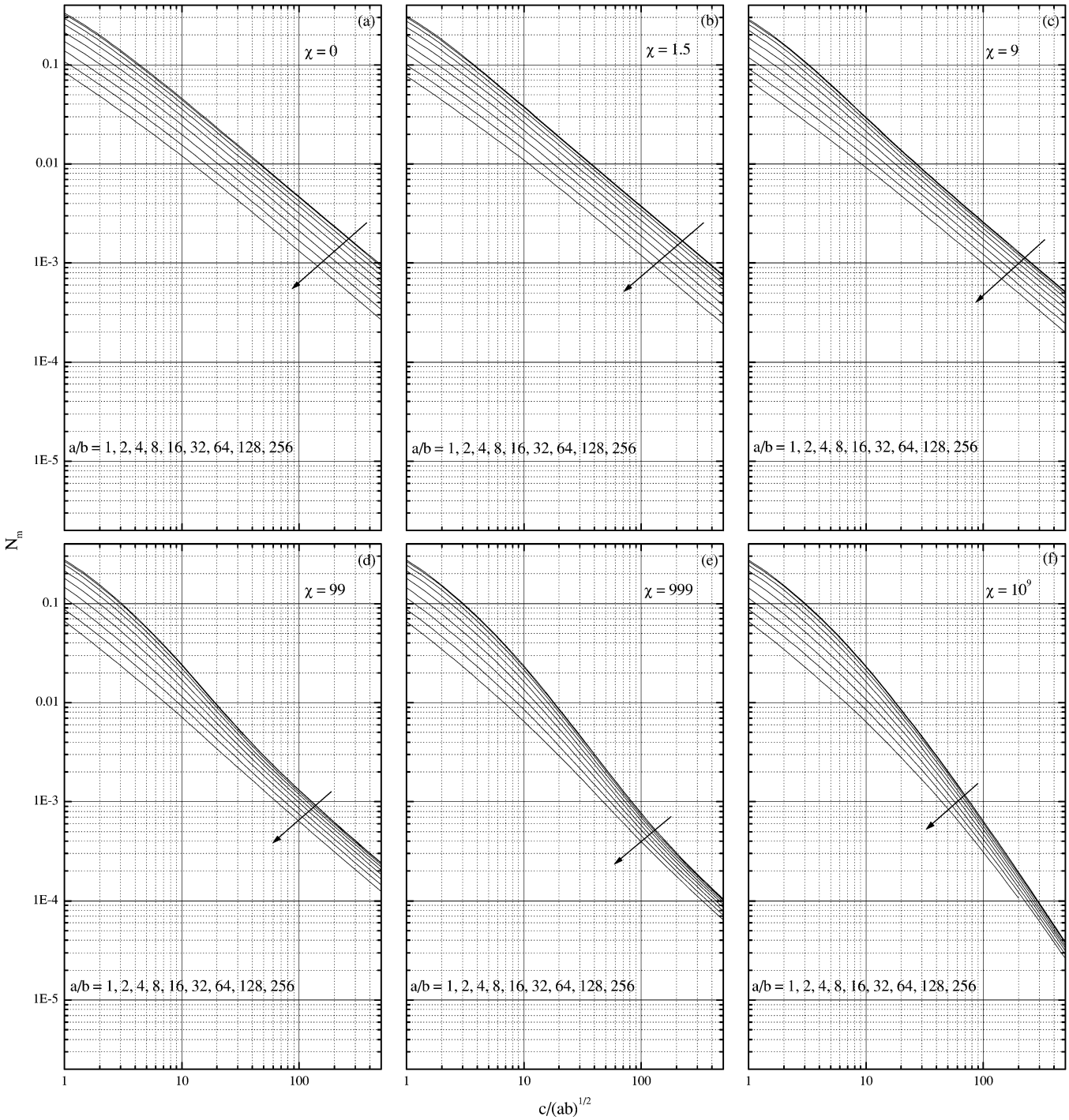

Fig. 2. N_m along the $2c$ dimension as a function of $c/(ab)^{1/2}$ at $a/b = 1, 2, 4, 8, 16, 32, 64, 128$, and 256 for rectangular prisms $2a \times 2b \times 2c$ with $\chi = 0$ (a), 1.5 (b), 9 (c), 99 (d), 999 (e), and 10^9 (f). Arrows point in the direction of increasing a/b.

that at $\chi = 0$ with increasing $c/(ab)^{1/2}$ from 1 to 200, $N_m(a/b = 1)/N_m(a/b = 256)$ decreases slightly from 4.0 to 3.5 but $N_f(a/b = 1)/N_f(a/b = 256)$ decreases greatly from 6.7 to 1.0, showing a remarkable difference between N_m and N_f. With increasing χ to ∞, both pairs of numbers turn out to be 4.2 to 1.8 and 4.5 to 1.8, respectively, suggesting that the behavior of N_m becomes similar to that of N_f with increasing χ. In fact, we have at any large $c/(ab)^{1/2}$ and given a/b that $N_m \gg N_f$ at small χ and $N_m \approx N_f \approx N$ at large χ, N being the demagnetizing factor for a corresponding ellipsoid. This rule was used for the approximate estimation of $N_{f,m}$ of rectangular prisms in [7], when the number of accurate data points was very limited. In order to show their relation after the present calculations, a comparison among N_m, N_f, and N at $\chi \to \infty$ is shown in Fig. 4 for $a/b = 1, 32$, and 128.

B. The Accuracy of Calculated $N_{f,m}$.

A general rule for the accuracy of the calculated $N_{f,m}$ is that it decreases with increasing $\chi, c/(ab)^{1/2}$, and a/b. From Table I, we see that the error is less than 0.1% for all N_m data at $\chi \leq 9$,

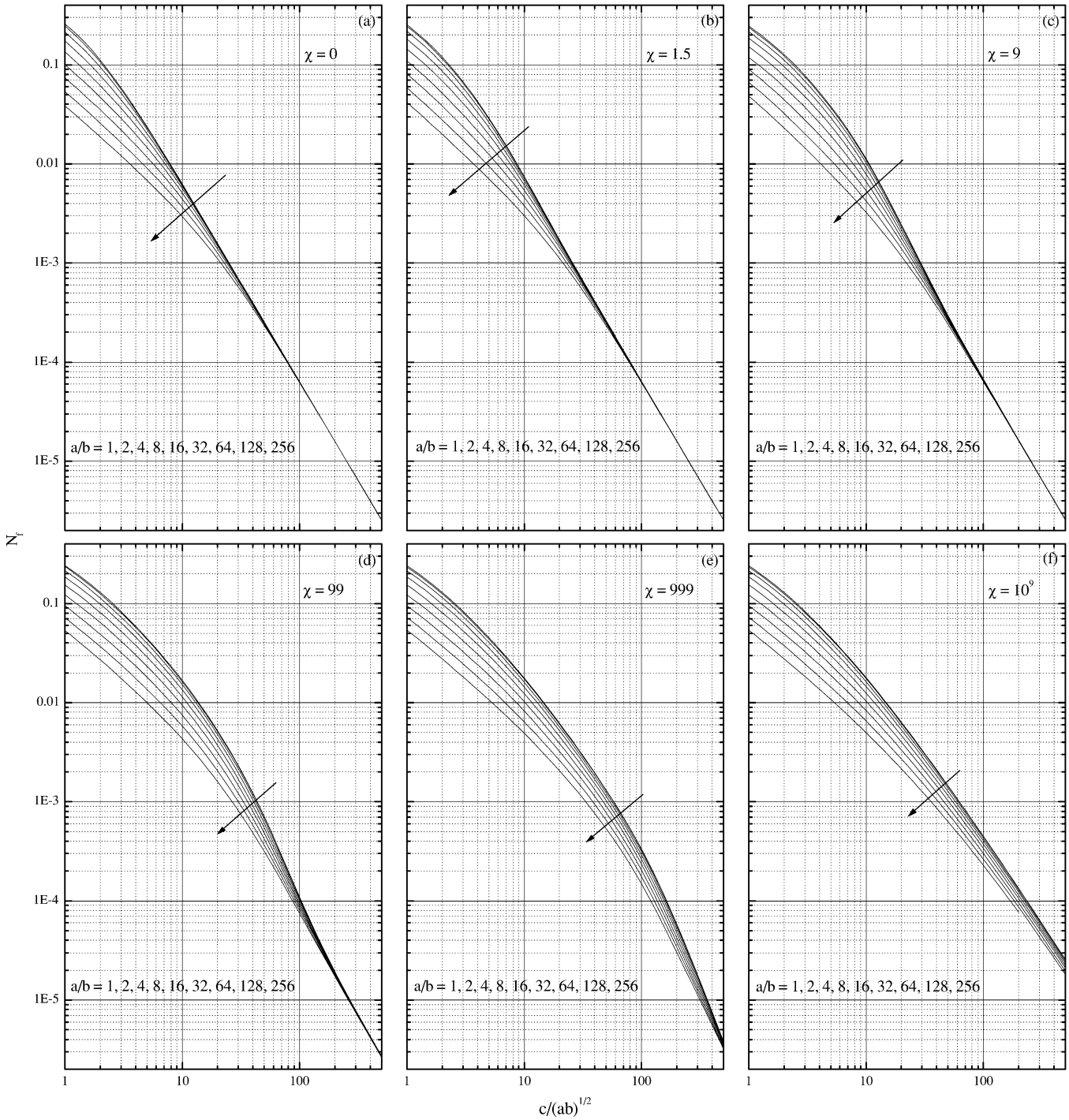

Fig. 3. N_f along the $2c$ dimension as a function of $c/(ab)^{1/2}$ at $a/b = 1, 2, 4, 8, 16, 32, 64, 128$, and 256 for rectangular prisms $2a \times 2b \times 2c$ with $\chi = 0$ (a), 1.5 (b), 9 (c), 99 (d), 999 (e), and 10^9 (f). Arrows point in the direction of increasing a/b.

and with increasing a/b from 1 to 256, the limiting $c/(ab)^{1/2}$ for 0.1% accuracy decreases from 500 to 10, from 100 to 5, and from 500 to 2 for $\chi = 99, 999$, and 10^9, respectively. There are only three points at $c/(ab)^{1/2} = 500$ or $a/b = 256$ where the error of N_m is larger than 1%. The accuracy of the calculated N_f is usually lower than that of N_m. From Table II, we see that the error is less than 0.1% for all N_f data at $\chi \leq 1.5$, and with increasing a/b from 1 to 256, the limiting $c/(ab)^{1/2}$ for 0.1% accuracy decreases from 500 to 100, from 50 to 5, from 100 to 2, and from 100 to 2 for $\chi = 9, 99, 999$, and 10^9, respectively. There are about 30 points at $c/(ab)^{1/2} = 500$ or $a/b = 256$ or $c/(ab)^{1/2} = 200, a/b = 128$ where the error of N_f is larger than 1%. Since the optimum element distribution at $\chi = 10^9$ has been used for $\chi = 9999$ and 10^5 without further optimization, the error of $N_{f,m}$ for both χ values is larger than that at $\chi = 999$ and 10^9.

We should mention that although the accuracy of the results may be improved by further optimizing the element distribution for each case, such an improvement will not be significant. With the used maximum n_p that corresponds to a reasonable com-

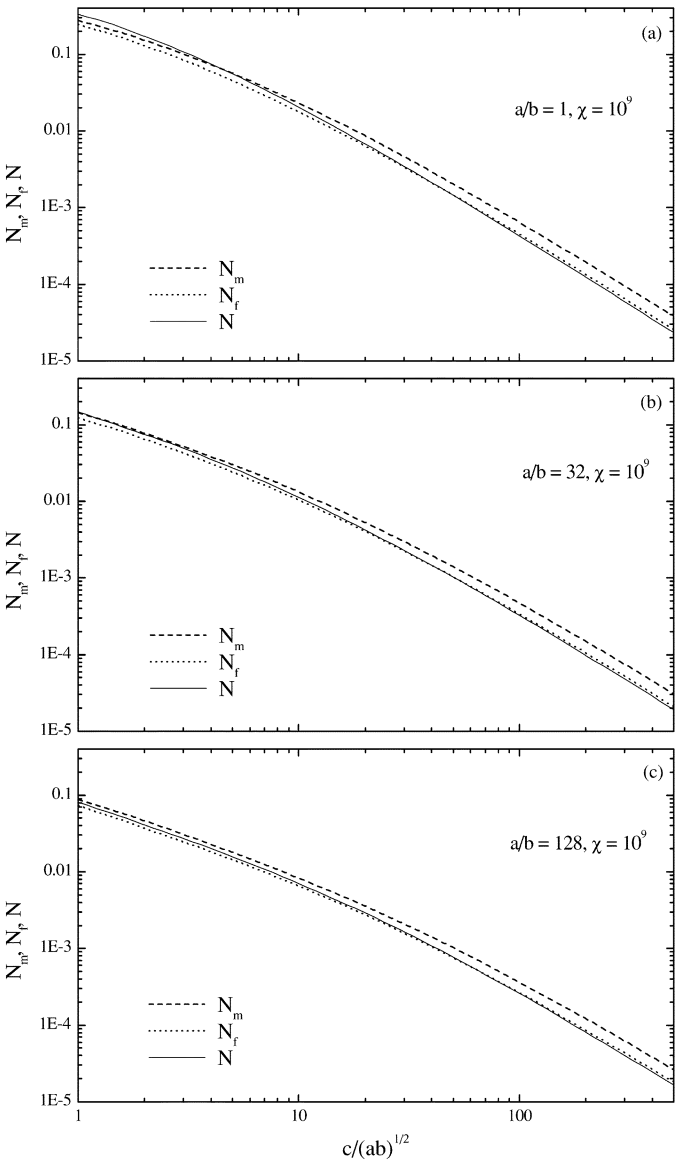

Fig. 4. Comparison of N_m and N_f versus $c/(ab)^{1/2}$ curves at $\chi = 10^9$ with demagnetizing factor N of ellipsoids of semi-axes a, b, and c for $a/b = 1, 32$, and 128 in (a), (b), and (c), respectively.

putation time, we cannot calculate $N_{f,m}$ for $c/(ab)^{1/2} > 500$ with an accuracy better than 1%. A further improvement in the accuracy would require a higher n_p and a greatly increased computation speed. The present high accuracy in a wide parameter region has been realized following all the points described in Section II after our long-term development, and we believe that further developments should still be proceeded in a heuristic way. Numerical calculation has been widely used in magnetostatics problems, and we feel that the calculation of $N_{f,m}$ for simple geometries can be a good test for treating complex systems, since the correctness and accuracy of the results can be well estimated for simple cases but not for the complex ones.

C. $N_{f,m}(\chi)$ for Arbitrary Aspect Ratios

The results of numerical calculations can only give discrete data points. Since accurate $N_{f,m}$ require a huge computation time, such data points should be reduced to a minimum number. As functions of $c/(ab)^{1/2}, a/b$, and χ, the number and distribution of the calculated $N_{f,m}$ points should ensure that accurate curves of $N_{f,m}$ versus $c/(ab)^{1/2}, a/b$, and χ be obtained from them. Plotting figures, we always connect a set of functional data points by a spline line in this paper. As explained earlier, with the chosen $c/(ab)^{1/2}$ values, $N_{f,m}[c/(ab)^{1/2}]$ curves can be plotted accurately in log–log scales for each pair of a/b and χ. After studying the conjugate relations in two-dimensional case [10], we know that $N_{f,m}$ versus the permeability $\mu/\mu_0 = \chi + 1$ is a log–log smooth function, so that a choice of $\mu/\mu_0 = 1, 10, 100, \ldots$ is reasonable. We have added one point at $\mu/\mu_0 = 2.5$, with which $N_{f,m}$ for weak magnetic materials can be obtained more accurately. The value of a/b is chosen in geometric progression growth of common factor 2, and we see from Figs. 2 and 3 that $N_{f,m}$ curves are quite uniformly placed when a/b is large, whereas they become denser when $a/b \to 1$. In fact, $a/b = p$ and $1/p$ are physically identical, and $N_{f,m}(a/b)$ is a parabolic curve centered at $a/b = 1$, which can be drawn accurately with the chosen values of a/b. Thus, with $N_{f,m}$ data listed in Tables I and II, $N_{f,m}$ for any intermediate values of $c/(ab)^{1/2}, a/b$, and χ can be obtained by interpolation with a satisfactory accuracy, and $N_{f,m}$ may also be obtained with less accuracy by extrapolation if their values are beyond the calculated range.

In actual magnetic measurements, the sample dimensions are fixed and one needs to get $N_{f,m}(\chi)$ at given values of $c/(ab)^{1/2}$ and a/b. As examples, we assume arbitrarily two samples to have $a/b = 1.5$ and 6 with a common $c/(ab)^{1/2} = 7.5$. All these values are not included in Tables I and II. The interpolation of N_m is performed as follows.

We first draw spline $N_m[c/(ab)^{1/2}]$ curves in log–log scales for $a/b = 1, 2, 4, 8$, and 16 and $\chi = 0, 1.5, 9, 99$, and 999 using data given in Table I, as demonstrated in Fig. 5(a)–(c). In order to get accurate spline curves, four $c/(ab)^{1/2}$ values around 7.5 are used. Drawing a vertical line at $c/(ab)^{1/2} = 7.5$, we obtain the y coordinate of its intersection point with each $N_m[c/(ab)^{1/2}]$ curve, so that N_m at $c/(ab)^{1/2} = 7.5$ and every pair of a/b and χ is obtained. We next draw spline $N_m(a/b)$ curve for each χ value and $c/(ab)^{1/2} = 7.5$, as shown in Fig. 5(d)–(f). Note that data points for $a/b = 1/2, 1/4, 1/8$, and $1/6$ are added when plotting spline curves, so that smooth symmetric parabolic curves are obtained. Drawing vertical lines at $a/b = 1.5$ and 6, we obtain $N_m(\chi)$ data by reading the y coordinate of the intersection points. These data points are connected by spline N_m versus $\chi + 1$ curves in Fig. 6, where they are compared with two nearby curves directly drawn using accurate data in Table I. Note that in Fig. 6, the N_m scale is set linear rather than logarithmic for ease of reading.

In the above cases all the directly calculated data points have error less than 0.1%, and the interpolated curves have added an error about 0.2%, as checked by extra direct calculations (see Table III).

D. Exemplified Application

The calculated $N_{f,m}$ versus $\chi, c/(ab)^{1/2}$, and a/b have various applications [3]. We introduce one that is a good represen-

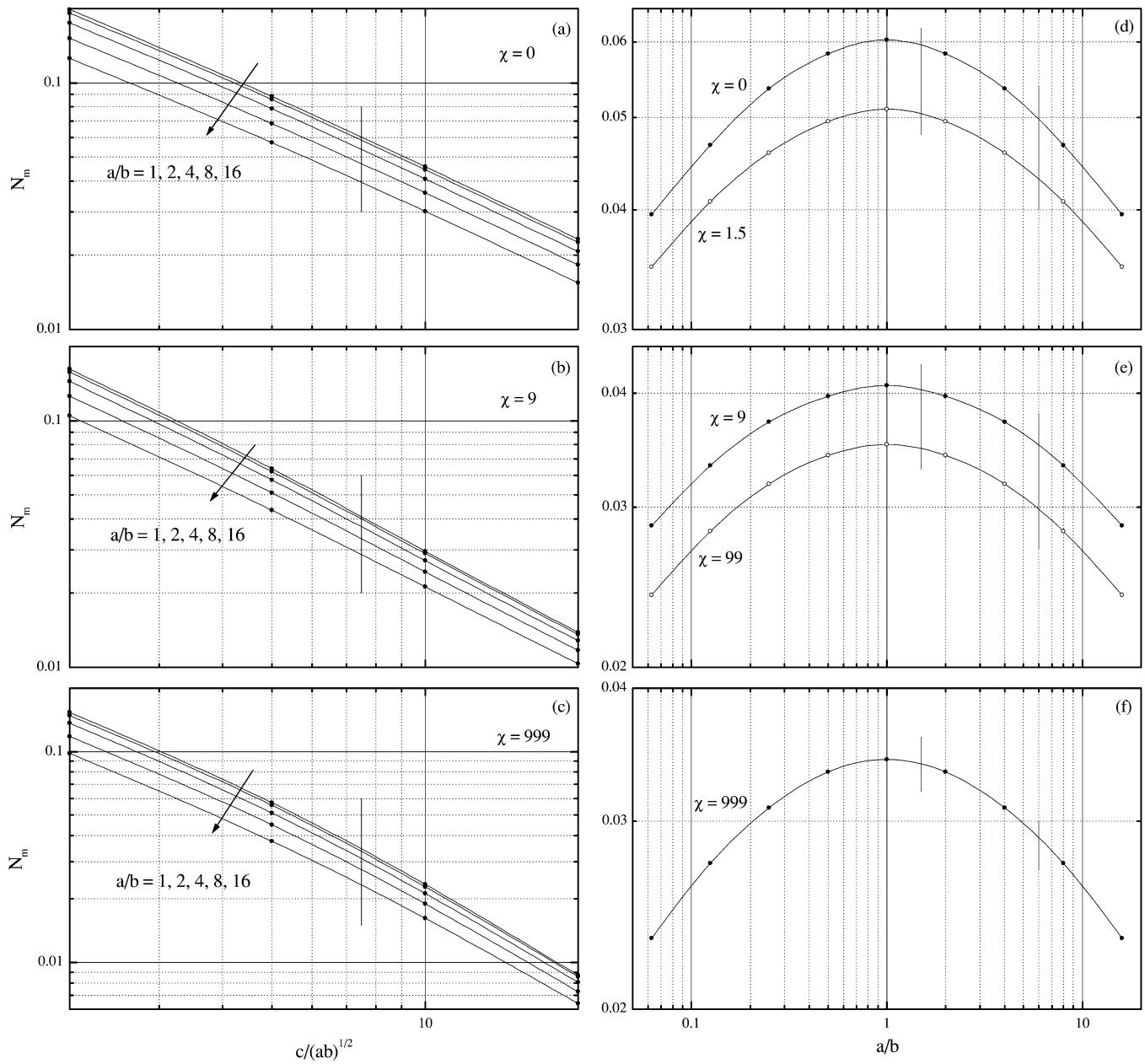

Fig. 5. Spline N_m versus $c/(ab)^{1/2}$ curves for $a/b = 1, 2, 4, 8$, and 16 and $\chi = 0$ (a), 9 (b), and 999 (c) connecting data points obtained from Table I. Spline N_m versus a/b curves for $c/(ab)^{1/2} = 7.5$ and $\chi = 0$ and 1.5 (d), 9 and 99 (e), and 999 (f). Arrows point in the direction of increasing a/b.

tative of the classical model of constant χ and requires very accurate N_m data.

It is known that for a ferromagnet at temperatures T slightly above the Curie temperature, T_C, the temperature dependent susceptibility follows:

$$\chi(T) = A(T/T_C - 1)^{-\gamma'} \tag{13}$$

where A and γ' are constants and the latter is referred to as the critical exponent. The value of γ' has been calculated using different models of magnetic structure. For example, it equals 1, 1.241, and 1.386 for the mean field, three-dimensional Ising, and three-dimensional Heisenberg models, respectively [15]. Using (13), we can determine precisely T_C and γ' from measured $\chi(T)$. The problem is that in the magnetometric measurements, the directly measured susceptibility is $\chi_{\rm ex} = M_{\rm vol}/H_a$ and it has to be corrected to χ using

$$1/\chi_{\rm ex} - N_{\rm m}(\chi) = 1/\chi. \tag{14}$$

In the past, such a correction was made assuming N_m to be constant, determined by the maximum $\chi_{\rm ex}$ in its field or T dependence [15]. According to (14), such determined N_m corresponds to its value at a certain high χ only, and it cannot be properly used for the correction since (13) involves χ that changes usually by two or three orders of magnitude.

To make a proper demagnetizing correction for the exemplified samples whose $N_m(\chi)$ functions are shown in Fig. 6, N_m and χ may be obtained iteratively. We expect that such a correction should give the value of γ' different from that using the traditional way, so that the physical conclusion might be changed

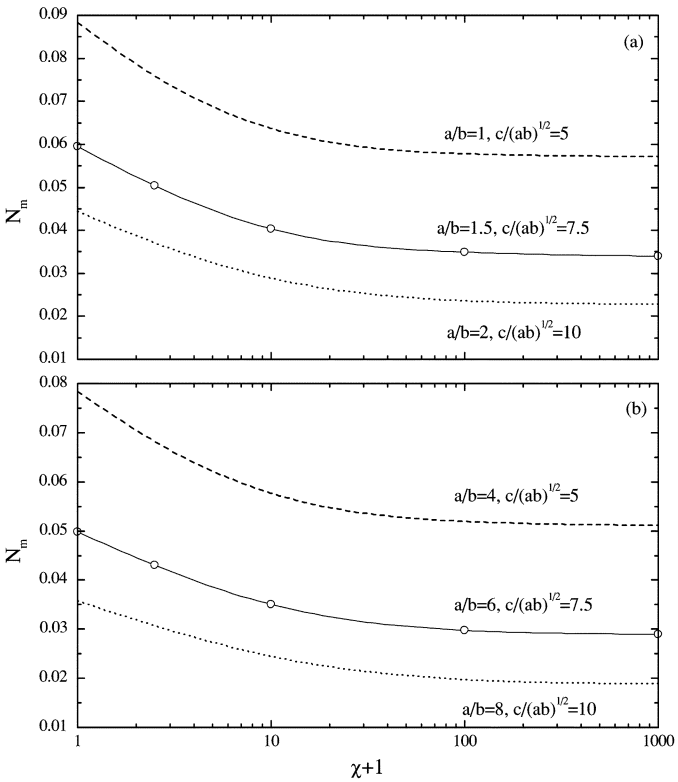

Fig. 6. Interpolated spline N_m versus $\chi+1$ curves for $c/(ab)^{1/2}=7.5$ and $a/b=1.5$ (a) and 6 (b) (solid lines). The dashed and dotted lines show accurate nearby curves drawn directly from data listed in Table I.

concerning the magnetic structure. The correction is performed using

$$1/\chi_{\rm ex} - N_{\rm m}^{(i)}\left(\chi^{(i-1)}\right) = 1/\chi^{(i)} \tag{15}$$

where the superscripts (i) $(i=1,2,3)$ denote the iteration step. When $i=1$, we set $\chi^{(0)}=\chi_{\rm ex}$ to get $N_m^{(1)}$ using the interpolated $N_m(\chi)$ curves in Fig. 6 and so $\chi^{(1)}$ using (15). We then use $\chi^{(1)}$ to get $N_{\rm m}^{(2)}$ and so $\chi^{(2)}$ and use $\chi^{(2)}$ to get $N_{\rm m}^{(3)}$ and so $\chi^{(3)}$ in a similar way. Assuming $\chi_{\rm ex}=2.00, 20.0$, and 26.0 for sample 1 with $a/b=1.5$ and $\chi_{\rm ex}=2.00, 20.0$, and 30.0 for sample 2 with $a/b=6$, the results are listed in Table III.

We see from Table III that both $N_m^{(i)}$ and $\chi^{(i)}$ become quite stable when $i\geq 2$, and therefore, three times of iterations are already enough and the final results can be taken as $N_m=(N_m^{(2)}+N_m^{(3)})/2$ and $\chi=(\chi^{(2)}+\chi^{(3)})/2$, as listed in Table III. Moreover, we have both $N_m(\chi_{\rm ex})/N_m(\chi)$ and $\chi/\chi_{\rm ex}$ to increase with increasing $\chi_{\rm ex}$. It is important to make an error analysis as follows.

Assuming the relative error of the measured $\chi_{\rm ex}$ and the calculated N_m is $\delta_{\chi_{\rm ex}}$ and δ_{N_m}, respectively, the relative error in the final χ calculated from (14) will be estimated by

$$\delta_\chi = \sqrt{\left(\delta_{\chi_{\rm ex}}\chi/\chi_{\rm ex}\right)^2+\left(\delta_{N_m}N_m\chi\right)^2} \tag{16}$$

if both partial errors are independent to each other. We see from (16) that δ_χ is greater than $\delta_{\chi_{\rm ex}}$ at least by a factor $\chi/\chi_{\rm ex}$, and the error in N_m gives an additional contribution to the error of χ if χ is large. Assuming $\delta_{\chi_{\rm ex}}=1\%$ and $\delta_{N_m}=0.3\%, \delta_\chi$ will increase from 1.1% to ~9% with increasing $\chi_{\rm ex}$ for the two samples in Table III. Thus, we conclude that in order to get χ with a reasonable accuracy, $\chi_{\rm ex}$ and $N_m(\chi)$ should be very accurate and $c/(ab)^{1/2}$ should be so large that $\chi/\chi_{\rm ex}$ is not too large.

V. Conclusion

For rectangular prisms of dimensions $2a\times 2b\times 2c$ with constant material susceptibility χ, we have calculated their fluxmetric and magnetometric demagnetizing factors $N_{f,m}$ along the $2c$ axis as functions of the values of χ and aspect ratios $c/(ab)^{1/2}$ and a/b. The results are listed in Tables I and II with 620 points in a parameter region of $\chi\geq 0, 1\leq c/(ab)^{1/2}\leq 500$, and $1\leq a/b\leq 256$. The error of $N_{f,m}$ is less than 1% for more than 95% of points, and it decreases to less than 0.01% with decreasing $\chi, c/(ab)^{1/2}$, and a/b. Since the distribution of the calculation points is well designed, $N_{f,m}$ for any values of parameters in the calculated region may be conveniently obtained by interpolations using spline lines with an satisfactory additional error of about 0.2%. Our results can be very useful for high quality magnetic measurements and accurate quantitative studies of magnetic materials.

Appendix
Summary of Quantities Used in the Paper

The studied body is a rectangular prism with a constant material susceptibility χ [or constant material permeability $\mu=(1+\chi)\mu_0$] centered at the origin and having dimensions $2a, 2b$, and $2c$ along the x, y, and z axes, respectively, in a uniform applied magnetic field $\mathbf{H}_a$ in the z direction.

Magnetic field $\mathbf{H}=\mathbf{H}_a+\mathbf{H}_d, \mathbf{H}_d$ being the demagnetizing field produced by magnetic poles in the prism and magnetization $\mathbf{M}=\chi\mathbf{H}$. Because the magnetic flux density $\mathbf{B}=\mu_0(\mathbf{M}+\mathbf{H})=\mu_0(1+1/\chi)\mathbf{M}$ and $\nabla\cdot\mathbf{B}=0$, we have $\nabla\cdot\mathbf{M}=0$ in the prism, so that magnetic poles are present on the surface only and are characterized by surface magnetic pole density $\sigma\equiv\mu_0\mathbf{M}\cdot\mathbf{e}$, where $\mathbf{e}$ is the outward unit vector normal to the surface.

Since $\mathbf{H}_d$ and $\mathbf{M}$ are generally nonuniform, we use $\mathbf{H}_{d,\rm av}$ and $\mathbf{M}_{\rm av}$ to stand for their average in general. H_a is the z component of $\mathbf{H}_a$. $H_{d,\rm mid}$ and $M_{d,\rm mid}$ are the z component of $\mathbf{H}_{d,\rm av}$ and $\mathbf{M}_{\rm av}$ when the average is made over the $z=0$ midplane. $H_{d,\rm vol}$ and $M_{d,\rm vol}$ are the z component of $\mathbf{H}_{d,\rm av}$ and $\mathbf{M}_{\rm av}$ when the average is made over the entire volume. Since these average quantities are generally used for both the ideal correct values and calculated values with some error, we redefine $M^*_{d,\rm mid,vol}$ and $H^*_{d,\rm mid,vol}$ to be the ideal correct values when both types of values appear in (12). $h^i_{z,\rm mid}$ and $h^i_{z,\rm vol}$ are the midplane average and volume average of the z component of the $\mathbf{H}_d$ per unit σ^i/μ_0 generated by the ith element in the region of $x,y,z>0$.

N is demagnetizing factor for ellipsoid along a principal axis. $N_{\rm av}$ is average demagnetizing factor in general. N_f is fluxmetric demagnetizing factor, i.e., and $N_{\rm av}$ when the average is made over the midplane. N_m is magnetometric demagnetizing factor, i.e., and $N_{\rm av}$ when the average is made over the entire volume. $N^s_{f,m}$ are $N_{f,m}$ calculated using "surface method" through $M_{\rm mis,vol}$. $N^v_{f,m}$ are $N_{f,m}$ calculated using

TABLE III
DETERMINATION OF N_m AND χ FROM THE MEASURED SAMPLE DIMENSIONS AND $\chi_{\rm ex}$. DIRECTLY CALCULATED N_m ARE WRITTEN WITHIN PARENTHESES

Sample No.	1			2		
$c/(ab)^{1/2}$	7.5			7.5		
a/b	1.5			6		
$\chi^{(0)}=\chi_{\rm ex}$	2.00	20.0	26.0	2.00	20.0	30.0
$N_m^{(1)}$	0.0487 (0.04866)	0.0374 (0.03747)	0.0368	0.0418 (0.04174)	0.0323 (0.03233)	0.0315
$\chi^{(1)}$	2.22	79.4	602	2.18	56.5	566
$N_m^{(2)}$	0.0481	0.0351	0.0341	0.0414	0.0304	0.0290
$\chi^{(2)}$	2.21	67.1	231	2.18	51.0	232
$N_m^{(3)}$	0.0481	0.0351	0.0343 (0.03433)	0.0414	0.0306	0.0293 (0.02930)
$\chi^{(3)}$	2.21	67.1	240	2.18	51.5	248
N_m	0.0481	0.0351	0.0342	0.0414	0.0305	0.0291
χ	2.21	67.1	235	2.18	51.2	240

"volume method" through $H_{d,\rm mis,vol}$. $N_{f,m}^c$ are $N_{f,m}$ corrected using (11) from $N_{f,m}^s$ and $N_{f,m}^v$.

$\chi_{\rm ex}\equiv M_{\rm vol}/H_a$ is external susceptibility.

x_i, y_i, and z_i are used for the center coordinates of the ith element; in the region of $x, y, x > 0$, these coordinates are (x_i, y_i, c), (a, y_i, z_i), or (x_i, b, z_i). $\Delta x, \Delta y$, and Δz are element size along the x, y, and z axes, respectively. $\Delta\sigma_x, \Delta\sigma_y$, and $\Delta\sigma_z$ are the σ increments used for calculating element divisions along the x, y, and z axes, respectively, from (3)–(5). $2n_x, 2n_y$, and $2n_z+1$ are the division numbers along the x, y, and z axes, respectively. $n_p\equiv n_xn_y+n_xn_z+n_yn_z$. n is the total element number.

$\delta_\chi, \delta_{\chi_{\rm ex}}$, and δ_{N_m} are the relative error in $\chi, \chi_{\rm ex}$, and N_m, respectively.

ACKNOWLEDGMENT

This work was supported by Spanish Ministerio de Educación y Ciencia Project Number FIS2004-02792, Catalan Projects SGR2001-00189, and CeRMAE. E. Pardo acknowledges the support of DURSI from the Generalitat de Catalunya. The authors thank the reviewers for their interest in the paper and valuable suggestions for its improvement.

REFERENCES

[1] R. M. Bozorth, *Ferromagnetism*, New York: Wiley, 2003, pp. 843–861.
[2] D.-X. Chen, *Physical Bases of Magnetic Measurements*. Beijing, China: China Mechanical Industry, 1985, pp. 175–206.
[3] D.-X. Chen, J. A. Brug, and R. B. Goldfarb, "Demagnetizing factors for cylinders," *IEEE Trans. Magn.*, vol. 27, no. 4, pp. 3601–3619, Jul. 1991.
[4] J. A. Osborn, "Demagnetizing factors of the general ellipsoid," *Phys. Rev.*, vol. 67, pp. 351–357, Jun. 1945.
[5] P. Rhodes and G. Rowlands, "Demagnetising energies of uniformly magnetized rectangular blocks," in *Proc. Leeds Phil. Lit. Soc.*, vol. 6, 1954, pp. 191–210.
[6] R. I. Joseph, "Ballistic demagnetizing factor in uniformly magnetized rectangular prisms," *J. Appl. Phys.*, vol. 38, pp. 2405–2406, 1967.
[7] D.-X. Chen, E. Pardo, and A. Sanchez, "Demagnetizing factors of rectangular prisms and ellipsoids," *IEEE Trans. Magn.*, vol. 38, no. 4, pp. 1742–1752, Jul. 2002.
[8] W. F. Brown, Jr., *Magnetostatic Principles in Ferromagnetism*. Amsterdam, The Netherlands: North-Holland, 1962, pp. 187–192.
[9] D.-X. Chen, C. Prados, E. Pardo, A. Sanchez, and A. Hernando, "Transverse demagnetizing factors of long rectangular bars: I. Analytical expressions for extreme values of susceptibility," *J. Appl. Phys.*, vol. 91, pp. 5254–5259, Apr. 2002.
[10] E. Pardo, A. Sanchez, and D.-X. Chen, "Transverse demagnetizing factors of long rectangular bars: II. Numerical calculations for arbitrary susceptibility," *J. Appl. Phys.*, vol. 91, pp. 5260–5267, Apr. 2002.
[11] E. Pardo, D.-X. Chen, and A. Sanchez, "Demagnetizing factors of square bars," *IEEE Trans. Magn.*, vol. 40, no. 3, pp. 1491–1499, May 2004.
[12] ——, "Demagnetizing factors for completely shielded rectangular prisms," *J. Appl. Phys.*, vol. 96, pp. 5365–5369, Nov. 2004.
[13] T. L. Templeton and A. S. Arrott, "Magnetostatics of rods and bars of ideally soft ferromagnetic materials," *IEEE Trans. Magn.*, vol. 23, no. 5, pp. 2650–2652, Sep. 1987.
[14] W. H. Press *et al.*, *Numerical Recipes in C*. Cambridge, U.K.: Cambridge Univ. Press, 1992.
[15] M. Seeger, S. N. Kaul, H. Kronmuller, and R. Reisser, "Asymptotic critical behavior of Ni," *Phys. Rev. B, Condens. Matter*, vol. 51, pp. 12 585–12594, 1995.

Manuscript received October 26, 2004; revised February 28, 2005.